

MASTER

On the multiscale finite volume method for the flow in porous media

Ermakov, K.

Award date:
2010

[Link to publication](#)

Disclaimer

This document contains a student thesis (bachelor's or master's), as authored by a student at Eindhoven University of Technology. Student theses are made available in the TU/e repository upon obtaining the required degree. The grade received is not published on the document as presented in the repository. The required complexity or quality of research of student theses may vary by program, and the required minimum study period may vary in duration.

General rights

Copyright and moral rights for the publications made accessible in the public portal are retained by the authors and/or other copyright owners and it is a condition of accessing publications that users recognise and abide by the legal requirements associated with these rights.

- Users may download and print one copy of any publication from the public portal for the purpose of private study or research.
- You may not further distribute the material or use it for any profit-making activity or commercial gain

Take down policy

If you believe that this document breaches copyright please contact us providing details, and we will remove access to the work immediately and investigate your claim.

Master Thesis

**On the Multiscale Finite Volume Method for the Flow in
Porous Media**

Konstantin Ermakov

Supervised by

PD Dr. Oleg Iliev

TU Kaiserslautern

August 16, 2010

Contents

1	Introduction	3
1.1	Motivation and state of the art	3
1.2	Aim of the thesis	4
1.3	Structure of the thesis	4
2	Problem formulation	5
2.1	Solving the problem on the fine scale	6
2.2	Notations and meshes for the MSFV method	9
2.3	The MSFV algorithm	9
3	Iterative MSFV method	13
3.1	Classical iMSFV method	13
3.2	Modification of the iMSFV method	16
4	Alternating Schwarz method	17
4.1	Additive Schwarz in the dual and multiplicative Schwarz in the primal coarse cells	17
4.2	Multiplicative Schwarz in both primal and dual coarse cells	19
5	The MSFV method in both dual and primal coarse cells	21
6	Numerical study of the methods for the flow in porous media	25
6.1	FV method on the fine scale	25
6.2	The MSFV method	26
6.3	Classical iMSFV method	28
6.4	Modification of iMSFV method	29
6.5	Alternating Schwarz method	30
6.5.1	Additive Schwarz in dual and multiplicative Schwarz in primal coarse cells	31
6.5.2	Multiplicative Schwarz in both dual and primal coarse cells	34
6.6	The MSFV method in both dual and primal coarse cells	36

Chapter 1

Introduction

1.1 Motivation and state of the art

The aim of the thesis is to develop and compare different numerical techniques for solving elliptic equations with highly heterogeneous coefficients. The heterogeneous nature of the coefficients, when varying at several scales, makes it difficult and sometimes impossible to solve the problem by standard numerical methods. In order to take into account all the fine scale variations, one needs to discretize the problem on the fine scale, which leads to a huge discretization matrix with all the usual difficulties arising from that.

A great number of natural and human made substances in the world are porous. For instance, rocks, soils, human bones, foams, ceramics, etc. are considered to be porous media. Their detailed description and, in particular, description of flows inside the porous media constitutes an important and at the same time challenging and difficult task. There is a number of applications, where the simulation of the flow in porous media is essential - water and gas filtration, hydrogeology, construction engineering, oil reservoir modeling, etc.

However, these simulations, if not done efficiently, take a lot of computer time and memory. An obvious way to solve the problem would be to discretize the initial equation to be able to represent all the fine scale variations of the solution. In this way it is, however, almost impossible to find a solution due to heterogeneity of the coefficients and their complex spacial distributions. Moreover, even if the problem is solved, in a number of cases one is not interested in all the fine scale details of the solution. In many cases one only needs coarse solution with some fine scale information in it.

For this reason a number of multiscale methods was introduced for the heterogeneous porous media flows. Currently, there are multiscale finite-element (MsFEM) methods [1], mixed multiscale finite-element (mixed MsFEM) methods [2], [3], [4] and multiscale finite volume (MSFV) methods [5], [7], where only the MMSFE and MSFV methods provide conservative fine scale velocity fields. All these methods can be used to find an approximation of the fine scale solution at a reduced computational cost.

1.2 Aim of the thesis

The main focus of this thesis will be in the MSFV method ([5], [6], [7]) and its modifications, e.g. iterative MSFV method ([8]). Apart from classical MSFV method it allows to iteratively update MSFV solutions on each step, and, moreover, it converges to the fine scale solution of the problem.

1.3 Structure of the thesis

In the next section problem formulation with all notations will be presented. Later in Section 2.3 the MSFV method will be explained. In chapter 3, iMSFV method together with its modifications will be presented. Alternating Schwarz methods will be considered in chapter 4. The iMSFV method in both dual and primal coarse cells will be presented in chapter 5. Numerical experiments will be considered in chapter 6 and, finally, the reader will find the conclusion of the thesis in chapter 7.

Chapter 2

Problem formulation

Consider the following elliptic problem

$$-\nabla \cdot (\boldsymbol{\lambda} \cdot \nabla p) = q \quad (2.1)$$

in the rectangular domain Ω with Dirichlet boundary conditions $p(\boldsymbol{x}) = g$ on the boundary $\partial\Omega$, with highly heterogeneous coefficients $\boldsymbol{\lambda}$. It describes saturated flow in porous media ([9], [10]).

Consider as an example an incompressible flow of two immiscible phases in heterogeneous porous media. The governing conservation equations are:

$$\phi \frac{\partial S_j}{\partial t} + \nabla \cdot \boldsymbol{u}_j = q_j, j = 1, 2 \quad (2.2)$$

where S_j is the saturation and \boldsymbol{u}_j is the velocity of the phase j . The porosity of the medium is ϕ , q_j is the source term. Now express the velocity as a function of pressure using the Darcy's law, i.e:

$$\boldsymbol{u}_j = -k \frac{k_j}{\mu_j} \nabla p, \quad (2.3)$$

where k , k_j and μ_j - absolute permeability, permeability and viscosity of the phase j , respectively.

Adding the two equations (2.2) and noting that $S_1 + S_2 = 1$, one obtains:

$$\nabla \boldsymbol{u} = q, \quad (2.4)$$

where $\boldsymbol{u} = \boldsymbol{u}_1 + \boldsymbol{u}_2$ and $q = q_1 + q_2$. Darcy's law for the total velocity is:

$$\boldsymbol{u} = -\lambda \nabla p, \quad (2.5)$$

with total mobility λ ,

$$\lambda = k \left(\frac{k_1}{\mu_1} + \frac{k_2}{\mu_2} \right)$$

The equation for pressure (2.1) is obtained by substitution of Eq. (2.5) into Eq. (2.4).

2.1 Solving the problem on the fine scale

In order to get used to the problem and notations, we will present the Finite Volume approach for solving the equation (2.1) on the fine scale.

We impose the fine grid ω , which resolves all the variations of the coefficients, on the domain Ω . The grid consist of X cells in x-direction and Y cells in y-direction. The size of the domain Ω is $L_x \times L_y$. Hence the size of each cell Ω_l is $h_x \times h_y = \frac{L_x}{X} \times \frac{L_y}{Y}$. The grid is cell-centered, i.e the points of the grid are located in the centers of the fine cells Ω_l , see Figure 2.1.

$$\omega = \left\{ (x_i, y_j) \mid x_0 = 0, x_1 = \frac{h_x}{2}, \dots, x_i = \frac{h_x}{2} + (i-1) \cdot h_x, \dots, x_{X+1} = L_x, \right. \\ \left. y_0 = 0, y_1 = \frac{h_y}{2}, \dots, y_j = \frac{h_y}{2} + (j-1) \cdot h_y, \dots, y_{Y+1} = L_y, i = 1, \dots, X, j = 1, \dots, Y \right\} \quad (2.6)$$

In order to obtain the finite volume discretization, one needs to integrate the initial equation (2.1) over all fine cells Ω_l , i.e:

$$- \int_{\Omega_l} \nabla \cdot (\lambda \cdot \nabla p) d\Omega = \int_{\Omega_l} q d\Omega \quad (2.7)$$

By applying Gauss theorem, one obtains:

$$- \int_{\partial\Omega_l} (\lambda \cdot \nabla p) \cdot \mathbf{n} d\Gamma = \int_{\Omega_l} q d\Omega \quad (2.8)$$

In order to find a discrete system, one needs to approximate the equation (2.8). The right-hand side can be easily approximated by the use of midpoint rule:

$$\int_{\Omega_l} q d\Omega = |\Omega_l| \cdot q_{i,j} = h_x h_y \cdot q_{i,j}, \quad (2.9)$$

where $|\Omega_l| = h_x h_y$ is the size of the fine cell Ω_l , and $q_{i,j}$ is the value of the source term q in the middle of the cell.

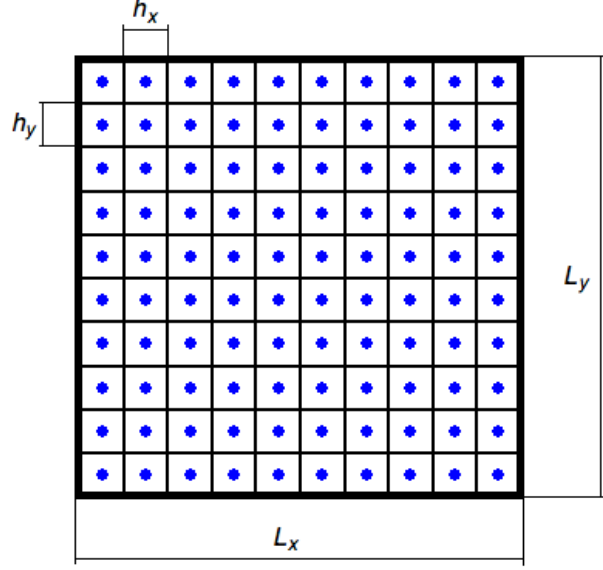


Figure 2.1: Domain Ω with imposed fine grid

Note that the left-hand side can be expressed as follows:

$$\begin{aligned} \int_{\partial\Omega_l} (\boldsymbol{\lambda} \cdot \nabla p) \cdot \mathbf{n} d\Gamma &= \int_{\Gamma_W} (\boldsymbol{\lambda} \cdot \nabla p) \cdot \mathbf{n}_W d\Gamma + \int_{\Gamma_E} (\boldsymbol{\lambda} \cdot \nabla p) \cdot \mathbf{n}_E d\Gamma \\ &+ \int_{\Gamma_N} (\boldsymbol{\lambda} \cdot \nabla p) \cdot \mathbf{n}_N d\Gamma + \int_{\Gamma_S} (\boldsymbol{\lambda} \cdot \nabla p) \cdot \mathbf{n}_S d\Gamma, \end{aligned} \quad (2.10)$$

where $\partial\Omega_l = \Gamma_E + \Gamma_W + \Gamma_N + \Gamma_S$, see Figure 2.2. Using midpoint rule for every integral in the expression above, one obtains:

$$\begin{aligned} &\lambda_{i+\frac{1}{2},j} \nabla p_{i+\frac{1}{2},j} \cdot h_y - \lambda_{i-\frac{1}{2},j} \nabla p_{i-\frac{1}{2},j} \cdot h_y \\ &+ \lambda_{i,j+\frac{1}{2}} \nabla p_{i,j+\frac{1}{2}} \cdot h_x - \lambda_{i,j-\frac{1}{2}} \nabla p_{i,j-\frac{1}{2}} \cdot h_x = -q_{i,j} \cdot h_x h_y \end{aligned} \quad (2.11)$$

and hence, approximating the values ∇p with central differences, one obtains the 5-point scheme, so that the equation (2.1) in the point (i, j) for the case when $2 \leq i \leq X$ and $2 \leq j \leq Y$ is approximated as follows:

$$\begin{aligned} &\frac{1}{h_x^2} \left(\lambda_{i-\frac{1}{2},j} p_{i-1,j} + \lambda_{i+\frac{1}{2},j} p_{i+1,j} \right) - \left(\frac{\lambda_{i-\frac{1}{2},j} + \lambda_{i+\frac{1}{2},j}}{h_x^2} + \frac{\lambda_{i,j-\frac{1}{2}} + \lambda_{i,j+\frac{1}{2}}}{h_y^2} \right) p_{i,j} \\ &+ \frac{1}{h_y^2} \left(\lambda_{i,j-\frac{1}{2}} p_{i,j-1} + \lambda_{i,j+\frac{1}{2}} p_{i,j+1} \right) = -q_{i,j} \end{aligned} \quad (2.12)$$

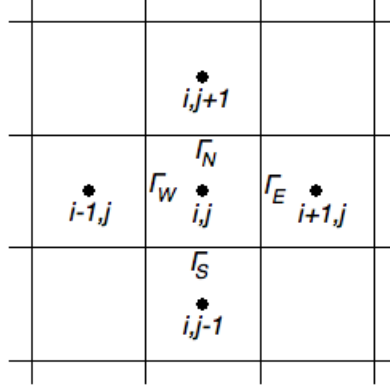


Figure 2.2: 5-point stencil in index notation

The stencil in index notation is represented in Figure 2.2.

The discretization near the left boundary (i.e when $i = 1$ and $2 \leq j \leq Y$) looks as follows:

$$\begin{aligned} \frac{1}{h_x^2} \left(2 \cdot \lambda_{0,j} p_{0,j} + \lambda_{\frac{3}{2},j} p_{2,j} \right) - \left(\frac{2 \cdot \lambda_{0,j} + \lambda_{\frac{3}{2},j}}{h_x^2} + \frac{\lambda_{1,j-\frac{1}{2}} + \lambda_{1,j+\frac{1}{2}}}{h_y^2} \right) p_{1,j} \\ + \frac{1}{h_y^2} \left(\lambda_{1,j-\frac{1}{2}} p_{1,j-1} + \lambda_{1,j+\frac{1}{2}} p_{1,j+1} \right) = -q_{1,j} \end{aligned} \quad (2.13)$$

The discretization near the right boundary (i.e when $i = X$ and $2 \leq j \leq Y$) looks as follows:

$$\begin{aligned} \frac{1}{h_x^2} \left(\lambda_{X-\frac{1}{2},j} p_{X-1,j} + 2 \cdot \lambda_{X+\frac{1}{2},j} p_{X+1,j} \right) - \left(\frac{\lambda_{X-\frac{1}{2},j} + 2 \cdot \lambda_{X+\frac{1}{2},j}}{h_x^2} + \frac{\lambda_{X,j-\frac{1}{2}} + \lambda_{X,j+\frac{1}{2}}}{h_y^2} \right) p_{X,j} \\ + \frac{1}{h_y^2} \left(\lambda_{X,j-\frac{1}{2}} p_{X,j-1} + \lambda_{X,j+\frac{1}{2}} p_{X,j+1} \right) = -q_{X,j} \end{aligned} \quad (2.14)$$

In the similar way one can discretize the equation near the lower ($j = 1$) and the upper ($j = Y$) boundaries.

Numerical results for this discretization will be presented in Section 6.1 of the thesis.

2.2 Notations and meshes for the MSFV method

The MSFV method requires 2 coarse grids to be imposed on the domain of interest Ω with the underlying fine grid. The first one is the primal coarse grid consisting of M cells $\bar{\Omega}_i$, the second one is the dual coarse grid consisting of N cells $\tilde{\Omega}_i$, as illustrated in Figure 2.3. Moreover

$$\bar{\Omega} = \bigcup_{i=1}^M \bar{\Omega}_i = \bigcup_{i=1}^N \tilde{\Omega}_i$$

The bold black line in the figure is the boundary of the domain Ω . The boundaries $\partial\bar{\Omega}_i$ of the primal coarse cells are represented by blue lines. The boundaries $\partial\tilde{\Omega}_i$ of the dual coarse cells are represented by dashed red lines. Note that each coarse cell (dual and primal) consists of several fine cells, and, in general, could be much coarser than the fine cell. The number of the fine cells per primal coarse cell is chosen to be odd, so that the center of the primal coarse cell coincides with the center of a fine cell. Moreover, each primal coarse cell contains one node \mathbf{x}_k (black dots) of the dual coarse cell, which is actually a center of the primal cell. All nodes \mathbf{x}_k belonging to one dual coarse cell $\tilde{\Omega}_i$ will be denoted as $\partial\partial\tilde{\Omega}_i$. Each dual coarse cell, except for the boundary ones, contains 4 points \mathbf{x}_k .

In the figure 2.4 the dual coarse cell $\tilde{\Omega}_i$ together with its boundaries is presented. The dashed red lines with the exception of the corners constitute the boundary $\partial\tilde{\Omega}_i$, the bold circles in the corners of the cell form $\partial\partial\tilde{\Omega}_i$. The inner part of the square cell is $\tilde{\Omega}_i$.

2.3 The MSFV algorithm

As it was originally introduced by P. Jenny in [8], the approximation p' to the fine pressure p_f can be described with the following expression:

$$p_f(\mathbf{x}) \approx p'(\mathbf{x}) = \sum_{i=1}^N \left(\sum_{k=1}^M \Phi_i^k(\mathbf{x}) \bar{p}_k + \Psi_i(\mathbf{x}) \right), \quad (2.15)$$

where:

- \bar{p}_k - pressure in the nodes \mathbf{x}_k ;
- Φ_i^k - basis functions;
- Ψ_i - correction functions.

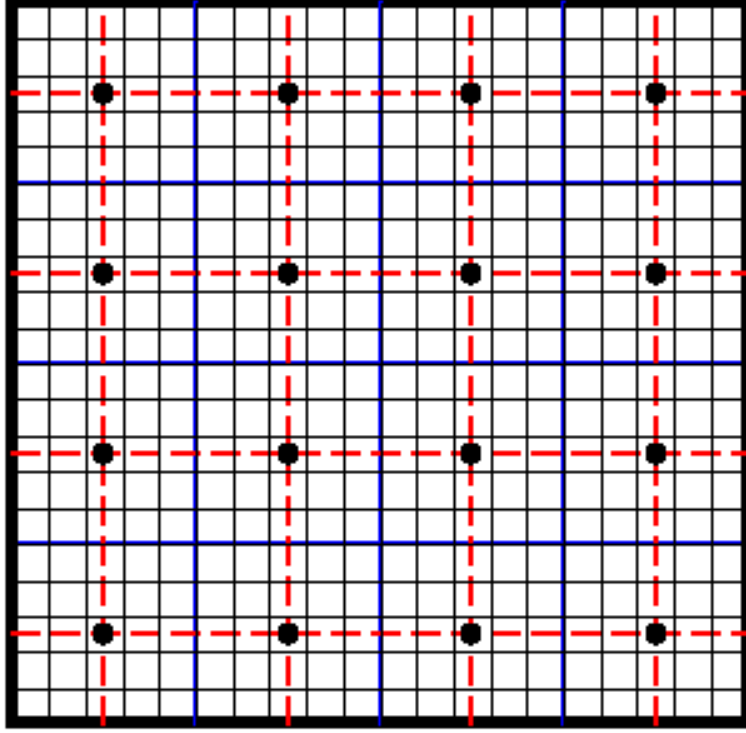


Figure 2.3: Domain Ω with imposed grids. The bold black line in the figure is the boundary of the domain Ω ; blue lines are the boundaries of the primal coarse cells $\partial\bar{\Omega}_i$; dashed red lines are the boundaries $\partial\tilde{\Omega}_i$ of the dual coarse cells; black nodes are the centers of the primal coarse cells.

The basis functions Φ and the correction functions Ψ are local numerical solutions (i.e. solutions on each dual coarse cell) of the problem (2.1) without and with right-hand side, respectively, with different boundary conditions. They should capture important fine scale features of the global problem ([11, 12]). To solve each local problem one must impose reduced problem boundary conditions on each $\partial\tilde{\Omega}_i$.

Note that the approximation p' mainly differs from the fine pressure p_f on the boundaries and the corners of the dual coarse cells, since the artificial localization boundary conditions are imposed there. For this reason, several methods will be introduced in the following parts of the thesis.

In other words, the following problems must be solved on each dual coarse cell:

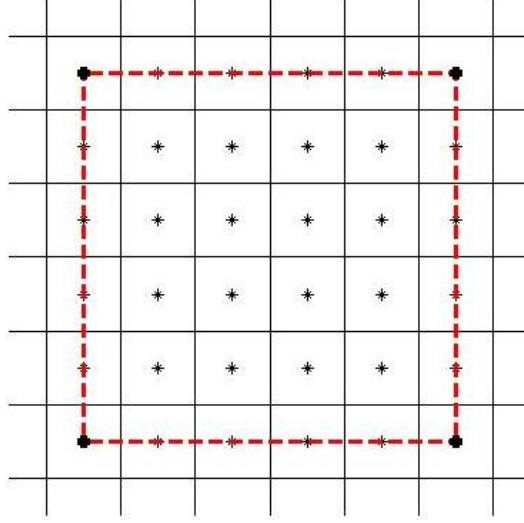


Figure 2.4: Dual coarse cell $\tilde{\Omega}_i$ together with it's boundaries. The dashed red lines with the exception of the corners constitute the boundary $\partial\tilde{\Omega}_i$; the bold circles in the corners of the cell form $\partial\partial\tilde{\Omega}_i$; the inner part of the square cell is $\tilde{\Omega}_i$.

1. For the basis functions:

$$-\nabla \cdot (\boldsymbol{\lambda} \cdot \nabla \Phi_i^k) = 0 \quad \text{in } \tilde{\Omega}_i \quad (2.16)$$

$$\frac{\partial}{\partial \tau} \boldsymbol{\lambda} \frac{\partial \Phi_i^k}{\partial \tau} = 0 \quad \text{on } \partial\tilde{\Omega}_i \setminus \partial\partial\tilde{\Omega}_i \quad (2.17)$$

$$\Phi_i^k(x_l) = \delta_{kl} \quad \text{for all } x_l \in \partial\partial\tilde{\Omega}_i \quad (2.18)$$

2. For the correction functions:

$$-\nabla \cdot (\boldsymbol{\lambda} \cdot \nabla \Psi_i) = q \quad \text{in } \tilde{\Omega}_i \quad (2.19)$$

$$-\frac{\partial}{\partial \tau} \boldsymbol{\lambda} \frac{\partial \Psi_i}{\partial \tau} = q \quad \text{on } \partial\tilde{\Omega}_i \setminus \partial\partial\tilde{\Omega}_i \quad (2.20)$$

$$\Psi_i(x_l) = 0 \quad \text{for all } x_l \in \partial\partial\tilde{\Omega}_i \quad (2.21)$$

In total, 5 problems should be solved on each dual coarse cell - 4 problems for basis functions and one problem for correction functions.

Note, that basis functions sum up to the solution of homogenized problem in each coarse cell. Adding the correction functions allows to take the inhomogeneities into account, since the approximation of the solution only by basis functions is inefficient, see [13].

The linear system for the coarse pressure values \bar{p}_k is derived as follows:

- Substitute expression (2.15) into equation (2.1).
- Integrate the resulting equation over $\bar{\Omega}_l$:

$$\begin{aligned} - \int_{\bar{\Omega}_l} \nabla \cdot (\boldsymbol{\lambda} \cdot \nabla p') d\Omega &= - \int_{\bar{\Omega}_l} \nabla \cdot \left(\boldsymbol{\lambda} \cdot \nabla \sum_{i=1}^N \left(\sum_{k=1}^M \Phi_i^k(\mathbf{x}) \bar{p}_k + \Psi_i(\mathbf{x}) \right) \right) d\Omega \\ &= \int_{\bar{\Omega}_l} q d\Omega \end{aligned} \quad (2.22)$$

for all $l \in [1, M]$

- By using the Gauss theorem:

$$\begin{aligned} & - \int_{\bar{\Omega}_l} \nabla \cdot \left(\boldsymbol{\lambda} \cdot \nabla \sum_{i=1}^N \left(\sum_{k=1}^M \Phi_i^k(\mathbf{x}) \bar{p}_k + \Psi_i(\mathbf{x}) \right) \right) d\Omega = \\ & - \int_{\partial \bar{\Omega}_l} \left(\boldsymbol{\lambda} \cdot \sum_{i=1}^N \left(\sum_{k=1}^M \bar{p}_k \nabla \Phi_i^k(\mathbf{x}) + \nabla \Psi_i(\mathbf{x}) \right) \right) \cdot \bar{\mathbf{n}}_l d\Gamma = \quad (2.23) \\ & \sum_{k=1}^M \bar{p}_k \sum_{i=1}^N \int_{\partial \bar{\Omega}_l} (-\boldsymbol{\lambda} \cdot \nabla \Phi_i^k(\mathbf{x})) \cdot \bar{\mathbf{n}}_l d\Gamma + \sum_{i=1}^N \int_{\partial \bar{\Omega}_l} (-\boldsymbol{\lambda} \cdot \nabla \Psi_i(\mathbf{x})) \cdot \bar{\mathbf{n}}_l d\Gamma = \int_{\bar{\Omega}_l} q d\Omega, \end{aligned}$$

where $\bar{\mathbf{n}}_l$ - the unit normal vector, pointing out of $\bar{\Omega}_l$

- Construct linear system

$$A_{lk} \bar{p}_k = b_l \quad (2.24)$$

for unknown \bar{p}_k where

$$A_{lk} = \sum_{i=1}^N \int_{\partial \bar{\Omega}_l} (-\boldsymbol{\lambda} \cdot \nabla \Phi_i^k(\mathbf{x})) \cdot \bar{\mathbf{n}}_l d\Gamma \quad (2.25)$$

$$b_l = \int_{\bar{\Omega}_l} q d\Omega - \sum_{i=1}^N \int_{\partial \bar{\Omega}_l} (-\boldsymbol{\lambda} \cdot \nabla \Psi_i(\mathbf{x})) \cdot \bar{\mathbf{n}}_l d\Gamma \quad (2.26)$$

As it can be seen from (2.25) and (2.26), the coarse matrix A , as well as the right-hand side b , contains the effects of the fine-scale fluxes across $\partial \bar{\Omega}_l$ induced by basis and correction functions, respectively.

Once the coarse pressure values \bar{p}_k are found, approximation of fine-scale pressure can be found from equation (2.15).

Chapter 3

Iterative MSFV method

3.1 Classical iMSFV method

The MSFV method gives a good approximation for the fine scale solution, but, unfortunately, it can not be used as a solver for the fine scale solution of the problem. That is why Iterative Multiscale Finite Volume Method (iMSFV) was introduced, which solution converges to the fine scale solution of the problem, see [5, 8, 14].

Consider now the fine scale discretization (2.12), (2.13) and (2.14) of the initial problem (2.1) as it was done in Section 2.1. Solving the system of equations obtained from this discretization is very challenging task and needs special iterative methods. Our goal is to present iterative method, based on the MSFV, which allows to compute the fine scale solution.

Compare fine scale approximation with the MSFV approximation in every point:

- On the boundaries of Ω both methods have Dirichlet boundary conditions.
- Inside the dual coarse cell $\tilde{\Omega}_i$ in the MSFV method the following equations are solved:

1. $-\nabla \cdot (\boldsymbol{\lambda} \cdot \nabla \Phi_i^k) = 0$ for the basis functions Φ_i^k .
2. $-\nabla \cdot (\boldsymbol{\lambda} \cdot \nabla \Psi_i) = q$ for the correction functions Ψ_i .

Summing up these equations with the help of (2.15) one obtains (2.1). Hence, in every point inside the dual coarse cells $\tilde{\Omega}_i$ the initial equation (2.1) is satisfied and the MSFV discretization coincides with the fine scale discretization (2.12), (2.13) and (2.14).

- On the boundaries of the dual coarse cells $\partial\tilde{\Omega}_i$ the following 1D problems are solved:

1. $\frac{\partial}{\partial \tau} \boldsymbol{\lambda} \frac{\partial \Phi_i^k}{\partial \tau} = 0$
2. $-\frac{\partial}{\partial \tau} \boldsymbol{\lambda} \frac{\partial \Psi_i}{\partial \tau} = q$

Hence, if one sums up the 2 equations above, one obtains $-\frac{\partial}{\partial \tau} \boldsymbol{\lambda} \frac{\partial p_i}{\partial \tau} = q$, i.e., in the MSFV method, the normal component of the initial equation (2.1) is not taken into account on the boundaries of the dual coarse cells.

- In the corners of the dual coarse cells $\partial\partial\tilde{\Omega}_i$ the equation (2.1) is not discretized explicitly on the fine scale. One has $\Phi_i^k(x_l) = \delta_{kl}$ for the basis functions Φ_i^k and $\Psi_i(x_l) = 0$ for the correction functions Ψ_i . There is, however, a coarse scale finite volume discretization and the corresponding linear system (2.24) for the pressure values in the points of $\partial\partial\tilde{\Omega}_i$.

The idea of iMSFV method, which comes out of the considerations above, is to take the solution of the MSFV method and use it for the normal component of the new local boundary conditions on the dual cells for correction functions, recalculate the correction functions and construct the new approximation of the solution, which should again be used for the new local boundary conditions. In this way, the initial equation (2.1) will be satisfied everywhere, including the boundaries of the dual coarse cells, except for the corners of the dual coarse cells.

More precisely, from the computational point of view it is more convenient that the coarse matrix A is computed only once in the beginning, i.e. the basis functions should not be changed from the ones computed in the MSFV method. As it was already noticed above the solution of the MSFV method mainly differs from the fine scale solution on the boundaries $\partial\tilde{\Omega}_i$ and $\partial\partial\tilde{\Omega}_i$ of the dual coarse cells, because the initial equation (2.1) is satisfied only inside the dual coarse cells $\tilde{\Omega}_i$, whereas the boundary conditions do not satisfy it. Hence, if the discretization on the boundaries of the dual coarse cells satisfied the equation (2.1), the MSFV solution would coincide with the fine scale solution.

Furthermore, as it follows from the considerations above, the normal component of the initial equation (2.1) is not taken into account on the boundaries. Hence, if

$$-\frac{\partial}{\partial \tau} \boldsymbol{\lambda} \frac{\partial \Psi_i}{\partial \tau} = q + \frac{\partial}{\partial n} \boldsymbol{\lambda} \frac{\partial}{\partial n} p_f$$

together with (2.17) (since the basis functions Φ_i^k should not be changed) then the basis functions Φ_i^k , $k = 1, \dots, M$ and the correction functions Ψ_i , $i = 1, \dots, N$ will sum up to the fine solution p_f . In other words, if the normal component of the fine pressure is taken into account on the boundaries, then the MSFV discretization will coincide with the fine scale discretization (with the exception of the points in

$\partial\partial\tilde{\Omega}_i$).

Hence, in order to improve the solution of the MSFV method iteratively, one needs to update the values of the correction functions Ψ_i , $i = 1, \dots, N$ on the boundaries of the dual coarse cells $\partial\tilde{\Omega}_i$ using the fine scale solution from the previous iteration.

This leads us to the following problem of the j -th iteration:

$$-\nabla \cdot (\boldsymbol{\lambda} \cdot \nabla \Psi_i) = q \quad \text{in } \tilde{\Omega}_i \quad (3.1)$$

$$-\frac{\partial}{\partial \tau} \boldsymbol{\lambda} \frac{\partial \Psi_i^{(j)}}{\partial \tau} = q + \frac{\partial}{\partial n} \boldsymbol{\lambda} \frac{\partial}{\partial n} S_1(p^{\text{iMSFV},(j-1)}, q) \quad \text{on } \partial\tilde{\Omega}_i \setminus \partial\partial\tilde{\Omega}_i \quad (3.2)$$

$$\Psi_i(x_l) = 0 \quad \text{for all } x_l \in \partial\partial\tilde{\Omega}_i \quad (3.3)$$

where S_1 is the smoothing operator, which will be described later.

As in the MSFV method, these problems should be solved on each dual coarse cell. After that, coarse system

$$A\bar{p}_k^{(j)} = b^{(j)}$$

should be solved to obtain new values of coarse pressure $\bar{p}_k^{(j)}$ in the coarse nodes \mathbf{x}_k . Then the iMSFV approximation on the j -th iteration can be written as

$$p^{\text{iMSFV},(j)}(\mathbf{x}) = S_2 \left[\sum_{i=1}^N \left(\sum_{k=1}^M \Phi_i^k(\mathbf{x}) \bar{p}_k^{(j)} + \Psi_i^{(j)}(\mathbf{x}) \right), q \right]$$

where S_1 and S_2 are smoothing operations that should be applied between iterations. Practical experiments show that Jacobi or Gauss-Seidel smoothings can be applied together with line relaxation ([8]). From the numerical studies one can conclude, that classical iMSFV method heavily depends on the type of smoothings and the number of smoothing steps between the iterations.

It will be shown in the numerical results, that in this implementation of iMSFV method converges to some approximation of the exact solution, where it stagnates. Moreover, the largest error is located on the $\partial\partial\tilde{\Omega}_i$ boundary, i.e in the centers of the primal coarse cells. As it was explained earlier, the initial equation (2.1) is satisfied everywhere on the fine scale with the exception of the points in $\partial\partial\tilde{\Omega}_i$; only the coarse scale finite volume approximation of the initial equation (2.1) is done in these points. Indeed, only conditions (2.18) and (2.21) are defined for the points in $\partial\partial\tilde{\Omega}_i$ on the fine scale. This fact leads us to the following section.

3.2 Modification of the iMSFV method

In the previous section it was shown, that the only points where the initial equation (2.1) is not satisfied, when classical iMSFV method is applied, are the points in $\partial\partial\tilde{\Omega}_i$. Hence, it should be possible to improve the method by explicitly writing the equation in these points for correction functions, instead of condition (3.3).

At before the grid consist of M primal coarse cells. Let us introduce a new notation for M , such that $M = M_x \times M_y$, i.e. the grid consists of M_x primal coarse cells in x -direction and M_y primal coarse cells in y -direction. Let $i_x = 1, \dots, M_x$ and $i_y = 1, \dots, M_y$. Moreover, let us introduce a new notation \tilde{p} , where $\sum_{k=1}^M \Phi^k(\mathbf{x}) \tilde{p}_k = \tilde{p}$.

Hence for the point (i_x, i_y) , $i_x = 1, \dots, M_x$, $i_y = 1, \dots, M_y$ one has:

$$-\nabla \cdot (\boldsymbol{\lambda} \cdot \nabla p_{i_x, i_y}) = -\nabla \cdot (\boldsymbol{\lambda} \cdot \nabla (\tilde{p}_{i_x, i_y} + \Psi_{i_x, i_y})) = q \quad (3.4)$$

This leads to the following implementation for the j -th iteration:

$$-\nabla \cdot (\boldsymbol{\lambda} \cdot \nabla \Psi_{i_x, i_y}^{(j)}) = q + \nabla \cdot (\boldsymbol{\lambda} \cdot \nabla \tilde{p}_{i_x, i_y}^{(j-1)}) \quad (3.5)$$

and then

$$\begin{aligned} \Psi_{i_x, i_y}^{(j)} = & \left(q + \nabla \cdot (\boldsymbol{\lambda} \cdot \nabla \tilde{p}_{i_x, i_y}^{(j-1)}) + \right. \\ & \left. \frac{1}{h_x^2} (\lambda_{i_x - \frac{1}{2}, i_y} \Psi_{i_x - 1, i_y}^{(j-1)} + \lambda_{i_x + \frac{1}{2}, i_y} \Psi_{i_x + 1, i_y}^{(j-1)}) + \frac{1}{h_y^2} (\lambda_{i_x, i_y - \frac{1}{2}} \Psi_{i_x, i_y - 1}^{(j-1)} + \lambda_{i_x, i_y + \frac{1}{2}} \Psi_{i_x, i_y + 1}^{(j-1)}) \right) / \\ & \left(\frac{\lambda_{i_x - \frac{1}{2}, i_y} + \lambda_{i_x + \frac{1}{2}, i_y}}{h_x^2} + \frac{\lambda_{i_x, i_y - \frac{1}{2}} + \lambda_{i_x, i_y + \frac{1}{2}}}{h_y^2} \right) \text{ for all } x_{i_x, i_y} \in \partial\partial\tilde{\Omega}_l, l = 1, \dots, N \end{aligned} \quad (3.6)$$

This modification of the iMSFV method, however, gives the same results as the usual iMSFV method. The calculated correction functions $\Psi^{(j)}$ and the coarse pressure values $\tilde{p}^{(j)}$ are different, but they sum up to the same approximation $p^{(j)}$ as in the iMSFV method. This phenomena have occurred for all the test cases considered, but the theoretical explanation is in the scope of the further research.

Chapter 4

Alternating Schwarz method

To get rid of the stagnation of the iMSFV method a combination of MSFV method and alternating Schwarz method was introduced. Alternating Schwarz method ([17], [18]) is designed to find the solution of an equation on a domain which is the union of a number of overlapping subdomains, by solving the equation on each of the subdomains, taking the values of the approximate solution obtained in the previous iteration as the boundary conditions.

Alternating Schwarz method is perfectly suitable to the problem of interest. First of all, the domain Ω can be represented as the two different unions of subdomains - primal coarse cells $\bar{\Omega}_i$ and dual coarse cells $\tilde{\Omega}_i$. Secondly, these cells have a large area of intersection, that is why the method should converge faster.

4.1 Additive Schwarz in the dual and multiplicative Schwarz in the primal coarse cells

Because of the construction of the dual grid, additive Schwarz method is a natural choice for solving the problem on the dual grid. On the very first iteration it takes the solution of the MSFV method as the boundary conditions for each of the dual coarse cell. Afterwards, it takes the solutions, obtained on the primal coarse cells by the multiplicative Schwarz method. The computations on the dual coarse cells can be easily parallelized, since the solutions on the dual cells do not depend on each other, but only on the solution obtained in the previous iteration. For some problems of high dimensions this approach could be crucial in speeding up the computations.

To avoid confusion introduce a new notation for the solution p' of the MSFV method from section 2.3: $p^{\text{MSFV}} = p'$. Then the solution algorithm looks as fol-

lows:

- Given the initial problem (2.1), find an approximation p^{MSFV} of the exact solution p_f by the MSFV method, where correction functions are not calculated and are taken to be zero.
- Discretize the equation (2.1) on the fine scale, i.e construct a linear system

$$A_f p = b_f, \quad (4.1)$$

where $p = p_f$ - the solution of the system.

- Calculate the residual $r_f = b_f - A_f p^{\text{MSFV}}$, where A_f is the fine matrix, obtained by discretization of the initial equation (2.1), b_f - vector of right hand side.
- Note that $p_f = p^{\text{MSFV}} + \delta_f$, then

$$A_f p_f = A_f (p^{\text{MSFV}} + \delta_f) = b_f, \quad (4.2)$$

hence

$$A_f \delta_f = b_f - A_f p^{\text{MSFV}} = r_f \quad (4.3)$$

To obtain the exact solution of (4.1) one needs to solve (4.3) for some correction δ_f and then sum up p^{MSFV} and δ_f to obtain p_f .

Solving (4.3) by classical techniques is, however, still difficult and time consuming, since there is still a huge fine scale matrix A . That is why alternating Schwarz method is necessary.

- In every dual coarse cell $\tilde{\Omega}_i$ solve the equation (4.3) in the internal part of $\tilde{\Omega}_i$ for the correction $\delta_f^{(\frac{1}{2})}$ with zero boundary conditions on $\partial\tilde{\Omega}_i$.
- In every primal coarse cell $\bar{\Omega}_i$ solve the equation (4.3) in the internal part of $\bar{\Omega}_i$ for the correction $\delta_f^{(1)}$ with the values of $\delta_f^{(\frac{1}{2})}$ as the boundary conditions.
- Continue solving (4.3) in dual and primal cells turn by turn using the values from the previous iterations as the boundary conditions until the required precision is achieved.

Note that since we have a cell centered grid, one needs to extend the primal cell when solving a local problem. In order to use values of δ_f from the previous iteration as the boundary conditions, one needs to take the values in the fine cells, neighboring to the primal coarse cell, see Fig. 4.1. The boundary of the primal coarse cell is the bold blue line, the points, where the boundary conditions are taken are shown by black dots.

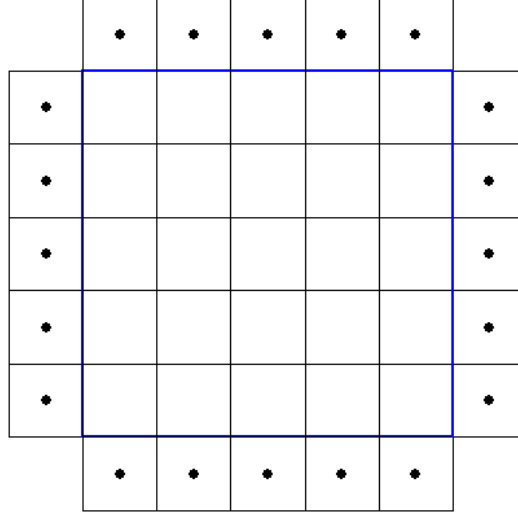


Figure 4.1: Primal coarse cell $\bar{\Omega}_i$. The boundary is the bold blue line; black dots - the points, where the boundary conditions are taken.

4.2 Multiplicative Schwarz in both primal and dual coarse cells

Another approach that can be used for solution of the initial problem (2.1) is the use of multiplicative Schwarz method ([18], [19]) for both types of coarse cells. For this reason the dual coarse cells are extended by one fine cell in each direction, and, hence, the solution obtained in these dual cells depend on each other. Moreover, the rate of convergence to the desired solution depends on the order of the computations (e.g. the method could converge faster if one starts from the upper-left dual cell, than from the lower-right). On the other hand, computations on the “new” dual coarse cells can not be parallelized as easy as it was done in the additive Schwarz method.

Figure 4.2 represents the “new” dual coarse cell, together with the old one. Solid black lines are the boundaries of the fine cells, stars are the centers of the fine cells. The dashed red line is the boundary of the original dual coarse cell, whereas solid blue line is the boundary of the new dual coarse cell.

In the next chapter another modification of the iMSFV method, which uses the idea of alternating Schwarz methods, will be presented.

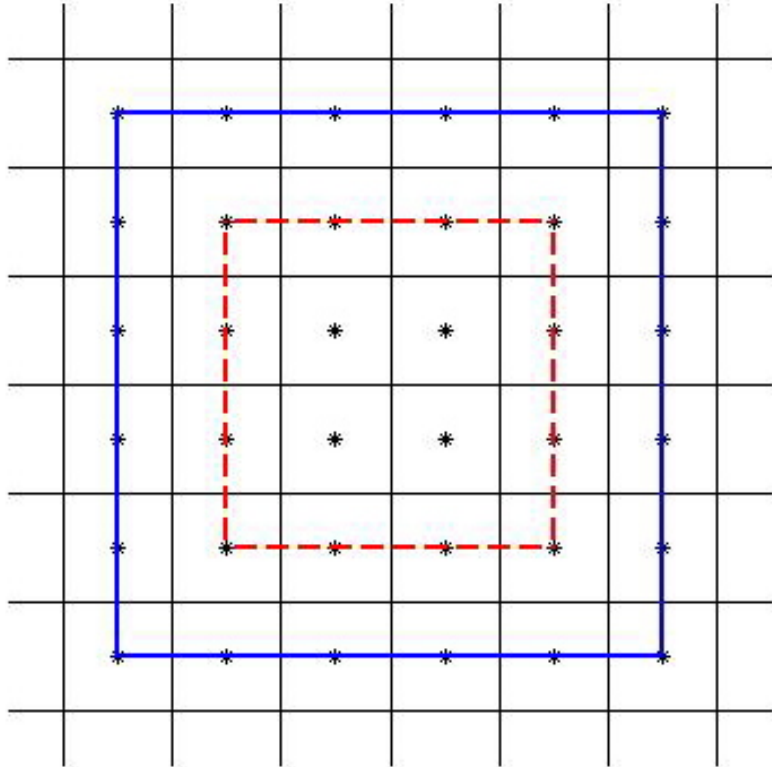


Figure 4.2: New coarse dual cell. The dashed red line is the boundary of the original dual coarse cell; solid blue line is the boundary of the new dual coarse cell.

Chapter 5

The MSFV method in both dual and primal coarse cells

All the methods given above provide a good approximation of the fine scale solution of the problem (2.1), however, as it will be shown in the numerical results, the rate of convergence is rather slow - sometimes it takes hundreds of iterations to converge to the desired tolerance. On the other hand, one knows, that the main error of the approximations is located on the boundaries of the dual coarse cells, that is why alternating Schwarz method was introduced for this kind of problems. However, the number of iterations needed by alternating Schwarz method heavily depends on the number of fine- and coarse cells constituting the domain.

The idea now is to take the concept of alternating Schwarz method and to combine it with the iMSFV framework. In all the methods above the MSFV method was only done in the dual coarse cells - in the iMSFV method in every iteration, and in alternating Schwarz only in the first iteration. Performing MSFV method both in the primal and the dual coarse cells should lead to the result similar to alternating Schwarz method (i.e. convergence to the fine scale solution of the problem), but without the drawbacks of this method (e.g. the convergence rate of the MSFV method should not depend on the number of coarse cells in the domain).

The solution algorithm looks as follows:

- As in the alternating Schwarz method the MSFV method is done in the first iteration to find an approximation of the fine scale solution, the correction functions are not calculated and are taken to be zero.
- The residual $r_f = b_f - A_f S_1(p^{\text{MSFV}}, q)$ is calculated, where A_f is the fine matrix, obtained by discretization of the initial equation (2.1), b_f - vector

of right hand side, S_1 is the smoothing operator, that must be applied after every iteration.

- Having the residual r_f and introducing the fine scale solution p_f as

$$p_f = p^{\text{MSFV}} + \delta_f, \quad (5.1)$$

one obtains the system of equations (4.3) for the values on the fine scale.

- Since the main error is concentrated on the boundaries of the dual coarse cells, the MSFV iteration is done on the primal coarse cells for the δ_f with r_f as the right hand side, again with correction functions taken to be zero. Hence, the following approximation for δ_f is used:

$$\delta_f \approx \delta'(\mathbf{x}) = \sum_{i=1}^M \left(\sum_{k=1}^N \Phi_i^k(\mathbf{x}) \bar{\delta}_f^k \right) \quad (5.2)$$

However, performing the MSFV iterations on the primal cells has some difficulties. In order to be able to construct the basis functions Φ_i^k one needs to introduce extra points on the boundaries of the primal cells. Initially, since the grid is cell-centered, there are no fine grid points on the boundaries of the primal coarse cells, since they consist of the boundaries of the fine cells.

The primal coarse cell together with the new points on the boundaries are introduced in Figure 5.1. The black lines are the boundaries of the fine cells, the bold blue lines are the boundaries of the primal coarse cells. Small black stars are the centers of the fine cells. The new points on the the boundaries are the bold black stars.

After introduction of the new fine grid points and solving the problem for the basis functions in the dual coarse cells, the coarse system similar to (2.24) is solved. The difference between the system (2.24) and the coarse system obtained on the primal cells is that now the coarse grid where the coarse system is solved, consists of the centers of the dual coarse cells, not the primal ones as before. Precisely,

$$\tilde{A}_{lk} \bar{\delta}_f^k = \tilde{b}_l \quad (5.3)$$

for unknown $\bar{\delta}_f^k$ where

$$\tilde{A}_{lk} = \sum_{i=1}^M \int_{\partial \tilde{\Omega}_l} (-\boldsymbol{\lambda} \cdot \nabla \Phi_i^k(\mathbf{x})) \cdot \tilde{\mathbf{n}}_l d\Gamma \quad (5.4)$$

$$\tilde{b}_l = \int_{\tilde{\Omega}_l} r_f d\Omega \quad (5.5)$$

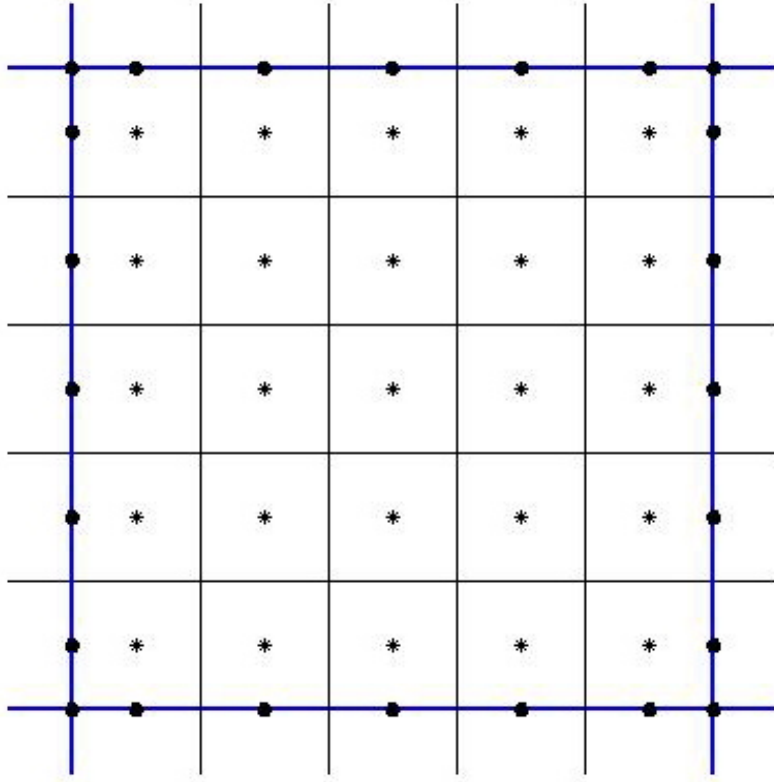


Figure 5.1: Primal cell together with newly introduced points on the boundary

- In the same way, as in the original MSFV method, the approximation δ' for the δ_f is calculated and, thus, the new approximation for the fine pressure p_f is obtained:

$$p^{\text{iMSFV},(\frac{1}{2})} = p^{\text{MSFV}} + \delta'$$

- Since the approximation δ' differs from the exact correction δ_f mainly on the boundaries of the primal coarse cells, the MSFV iteration should now be done in the dual coarse cells. Hence, the new residual $r_f^{(\frac{1}{2})}$ is calculated:

$$r_f^{(\frac{1}{2})} = b_f - A_f S_2(p^{\text{iMSFV},(\frac{1}{2})}, q), \quad (5.6)$$

the exact solution can be written as

$$p_f = p^{\text{iMSFV},(\frac{1}{2})} + \delta_f^{(\frac{1}{2})} \quad (5.7)$$

and, thus, the following system of equations for $\delta_f^{(\frac{1}{2})}$ can be constructed:

$$A_f \delta_f^{(\frac{1}{2})} = r_f^{(\frac{1}{2})} \quad (5.8)$$

- As before $\delta_f^{(\frac{1}{2})}$ can be approximated with the following expression:

$$\delta_f^{(\frac{1}{2})} \approx \delta'^{(\frac{1}{2})}(\mathbf{x}) = \sum_{i=1}^N \left(\sum_{k=1}^M \Phi_i^k(\mathbf{x}) \bar{\delta}_f^{k,(\frac{1}{2})} \right) \quad (5.9)$$

Note that, because the MSFV iteration is done in the dual coarse cells (not in the primal ones as in the previous iteration), the summation in the expression above is changed comparing to the expression (5.2)

- In the same way as it was explained earlier, the MSFV iteration is performed in the dual coarse cells, with correction functions Ψ_i taken to be zero. Coarse system similar to (2.24), but for the corrections $\delta'^{(\frac{1}{2})}$, is solved and the approximation of the $\delta_f^{(\frac{1}{2})}$ is obtained on the fine scale.
- Then one obtains the following improved approximation for the fine pressure p_f :

$$p^{\text{iMSFV},(1)} = p^{\text{iMSFV},(\frac{1}{2})} + \delta'^{(\frac{1}{2})}$$

- New residual $r_f^{(1)}$ is calculated and the process is repeated on the primal cells.

S_1 and S_2 are smoothing operations that should be applied between iterations. Numerical studies show that Jacobi or Gauss-Seidel line relaxation must be applied for the convergence of the method. However, the dependence of the method on the smoothing operations is much less comparing with the classical iMSFV method. For all the considered test cases, one step of Gauss-Seidel line relaxation between the iterations was enough to achieve good convergence results.

Thus, performing the MSFV iterations turn by turn on the primal and the dual coarse cells leads to quite sophisticated results, as it will be presented in the section 6.6 with the numerical study of this method.

Chapter 6

Numerical study of the methods for the flow in porous media

In this chapter numerical results for all the methods above will be presented. In all the problems the domain is $\Omega = (0, 1)^2$, if not mentioned the opposite. For the MSFV methods the grid is introduced as, for instance, $[5 \cdot 15 \times 5 \cdot 15]$ - it means, that the grid consists of 5 primal coarse cells in each direction and 15 fine cells in each primal coarse cell in each direction.

6.1 FV method on the fine scale

In the beginning of the chapter, the finite volume method on the fine scale is considered.

Consider the following system:

$$-\nabla \cdot ((2 + \sin(25x)) \cdot \nabla p) = -25 \cos(25x) \quad \text{in } \Omega \quad (6.1)$$

$$p = x \quad \text{on } \partial\Omega \quad (6.2)$$

$\Omega = (0, 1)^2$, the exact solution is $p = x$. The grid consists of $[150 \times 150]$ fine cells. For solving the arising linear system the conjugate gradient method is used, with the default Matlab tolerance $1 \cdot 10^{-6}$.

Without the preconditioner the method converges to the solution with the relative residual $9.8 \cdot 10^{-7}$ in 431 iterations. With the Jacobi preconditioner it converges in 354 iterations with the relative residual $9 \cdot 10^{-7}$. Relative residual with respect to the iteration number for both methods is presented in Figure 6.1. The solution, obtained by the method is presented in the Figure 6.2.

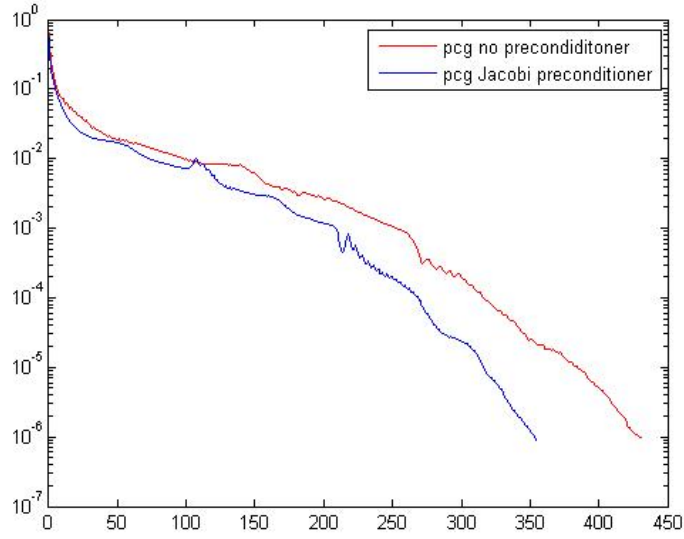


Figure 6.1: Relative residual with respect to the iteration number for the conjugate gradient method with and without preconditioner for system (6.1)-(6.2) with $[150 \times 150]$ grid

Now consider the grid $[300 \times 300]$. The conjugate gradient method without the preconditioner converges to the solution in 845 iterations, while the same method with Jacobi preconditioner converges to the solution in 686 iterations, see Figure 6.3.

6.2 The MSFV method

Consider the following simple system:

$$-\Delta p = 0 \quad \text{in } \Omega \quad (6.3)$$

$$p = x \quad \text{on } \partial\Omega \quad (6.4)$$

where $\Omega = (0, 1)^2$, the exact solution is $p = x$. The grid consists of $[5 \times 5]$ coarse cells and $[5 \cdot 15 \times 5 \cdot 15]$ fine cells.

The MSFV method calculates the solution with the relative residual $1.2 \cdot 10^{-15}$. Having in mind that precision of the version of Matlab, where the calculations took place, is $2.2 \cdot 10^{-16}$, one can say, that the MSFV method gives the exact solution

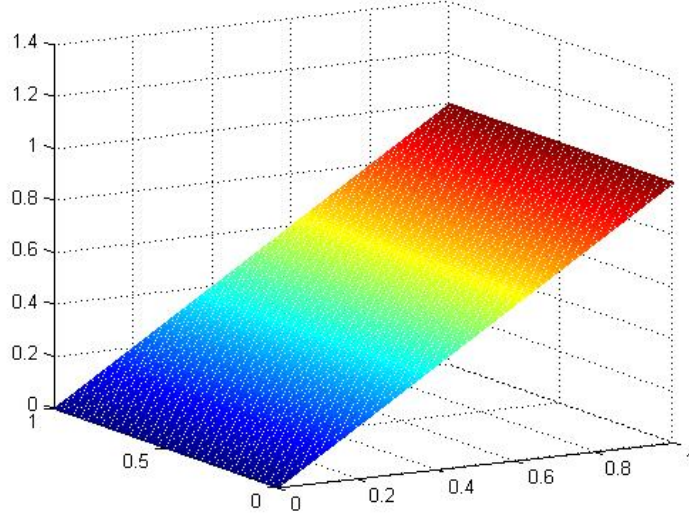


Figure 6.2: Solution of the system (6.1)-(6.2) obtained by the pcg method on the $[150 \times 150]$ grid

of this equation.

Consider another auxillary system, this time with high frequency of the coefficients, but still with smooth solution:

$$-\nabla \cdot ((2 + \sin(25y)) \cdot \nabla p) = 0 \quad \text{in } \Omega \quad (6.5)$$

$$p = x \quad \text{on } \partial\Omega \quad (6.6)$$

The exact solution is again $p = x$ and $\Omega = (0, 1)^2$. The grid consists of $[5 \cdot 15 \times 5 \cdot 15]$ fine cells.

The relative residual of the MSFV solution is $3.1 \cdot 10^{-15}$, which is still very close to the precision of Matlab.

Things change, however, with non-zero right-hand side. Consider the system (6.1)-(6.2) from the previous section.

The exact solution is $p = x$. The grid consists of $[5 \cdot 15 \times 5 \cdot 15]$ fine cells. In this case, the MSFV method only gives an approximation of the solution with the relative residual $4.8 \cdot 10^{-2}$. Approximation is shown in Figure 6.4.

Now increase the number of coarse cells - consider a grid with $[10 \times 10]$ coarse cells and $[15 \times 15]$ fine cell per coarse cell.

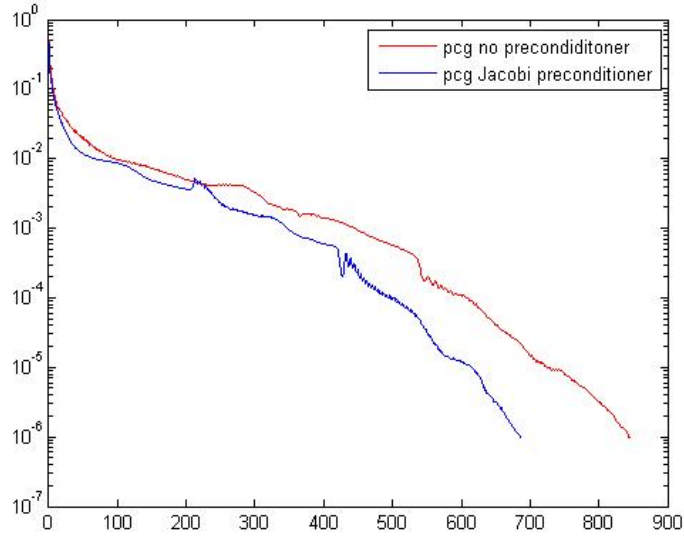


Figure 6.3: Relative residual with respect to the iteration number for the conjugate gradient method with and without preconditioner for system (6.1)-(6.2) with $[300 \times 300]$ grid

The relative residual decreases to $1.3 \cdot 10^{-2}$. The MSFV solution is presented in Figure 6.5.

Now instead if increasing the number of coarse cells, we will increase the number of fine cells, so that the grid consists of $[5 \cdot 25 \times 5 \cdot 25]$ fine cells.

The relative residual is $4.7 \cdot 10^{-2}$, which is only slightly less than for the case of $[15 \times 15]$ fine cells per coarse cell. The MSFV solution for this case is presented in Figure 6.6.

6.3 Classical iMSFV method

For iMSFV method consider the system of equations (6.1)-(6.2) from one of the previous examples.

The grid consists of $[5 \cdot 15 \times 5 \cdot 15]$ fine cells. After every iMSFV iteration 10 smoothing steps (Gauss-Seidel line relaxation) are performed. The method converges to the solution until iteration no. 11, where the convergence stops with the relative residual $1.8 \cdot 10^{-5}$. The difference between the exact solution $p = x$ and the approximation on the 11-th iteration is presented in Figure 6.7.

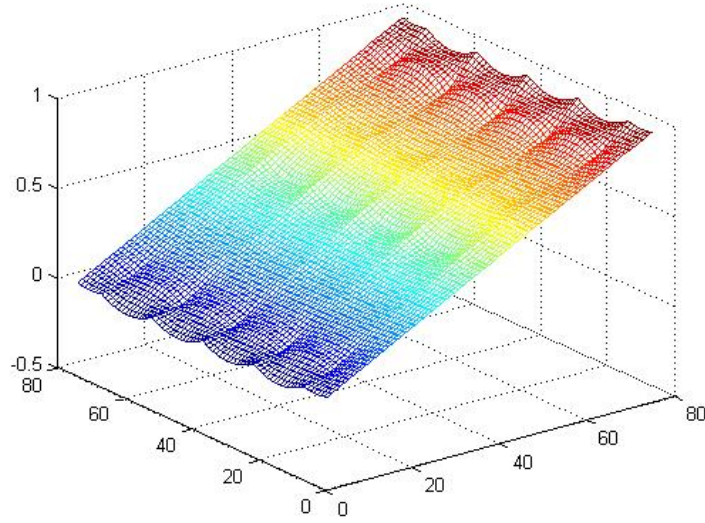


Figure 6.4: Approximation obtained by MSFV method with non-zero right-hand side and $[5 \cdot 15 \times 5 \cdot 15]$ grid

As one can see, the main error is located in the centers of primal coarse cells, i.e the points in $\partial\partial\tilde{\Omega}_i$ $i = 1, \dots, N$. The explanation to this fact is that in these points the initial equation (2.1) is never written down explicitly.

Classical iMSFV method heavily depends on the number and the type of smoothing steps between the iterations. In the considered example several Gauss-Seidel line relaxation steps were performed. In the Figure 6.8 the behavior of the iMSFV method for different number of smoothing steps is presented. As it can be seen there, for a small number of smoothing steps ($n = 2$ and $n = 5$) the method even diverge. For $n = 10$ and $n = 15$ the method converge until the the relative residual $1.8 \cdot 10^{-5}$ is reached and then it stagnates.

6.4 Modification of iMSFV method

In order to overcome the stagnation of the iMSFV method we have introduced the modified version of the iMSFV method. However, the results did not improve.

Consider the same system (6.1)-(6.2) of equations from the previous examples.

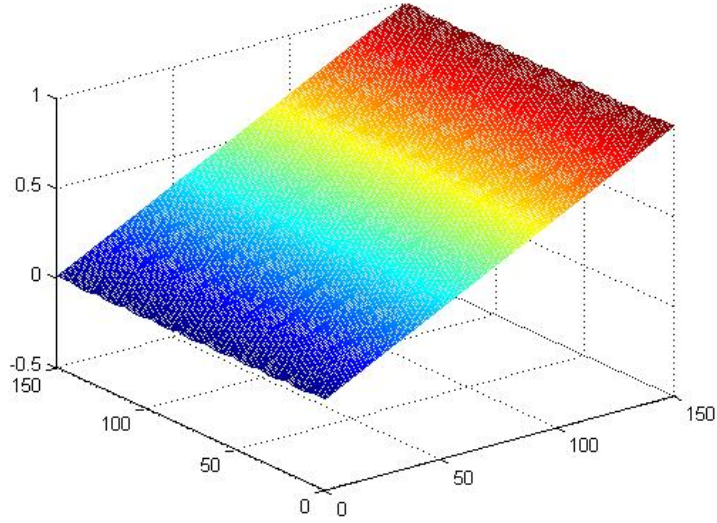


Figure 6.5: MSFV solution with non-zero right-hand side and $[10 \cdot 15 \times 10 \cdot 15]$ fine cells

The grid is the same as in the previous example, i.e. consists of $[5 \cdot 15 \times 5 \cdot 15]$ fine cells. As before, the method converges until the iteration no. 11, where the residual is $1.8 \cdot 10^{-5}$. The solution obtained by this method coincides with the solution obtained by classical iMSFV method. The only difference is in the values of $\bar{p}^{(k)}$ and $\Psi^{(k)}$, but their sum (fine scale pressure) stays the same.

6.5 Alternating Schwarz method

In this section we will present numerical results for 2 different implementations of alternating Schwarz method:

- Additive Schwarz in dual coarse cells and multiplicative Schwarz in primal coarse cells.
- Multiplicative Schwarz in dual coarse cells and also multiplicative Schwarz in primal coarse cells.

Both versions have their advantages and disadvantages - multiplicative Schwarz usually converges faster, but additive Schwarz is convenient for parallel computing.

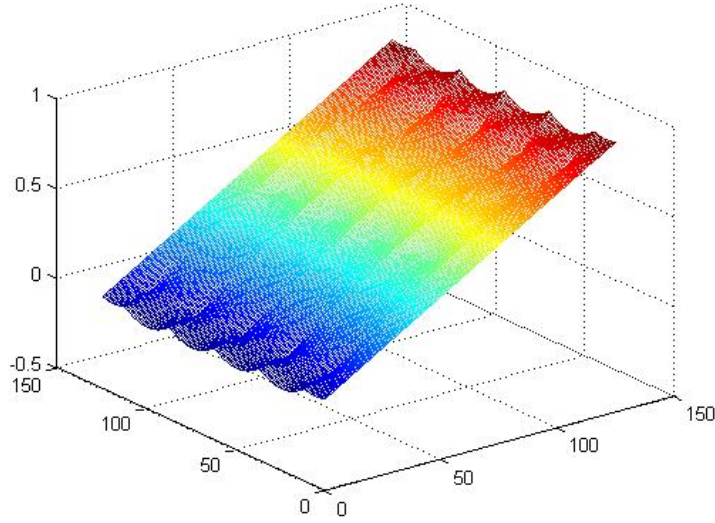


Figure 6.6: MSFV solution with non-zero right-hand side and $[5 \cdot 25 \times 5 \cdot 25]$ fine cells

6.5.1 Additive Schwarz in dual and multiplicative Schwarz in primal coarse cells

Consider the following equation:

$$-\Delta p = -2 \quad \text{in } \Omega \quad (6.7)$$

$$p = x^2 \quad \text{on } \partial\Omega \quad (6.8)$$

with the exact solution $p = x^2$.

Consider at first a relatively small grid with $[5 \cdot 5 \times 5 \cdot 5]$ fine cells. The desired tolerance is $1 \cdot 10^{-6}$. Alternating Schwarz method converges in 35 iterations. Since on every step we perform computations on both primal and dual cells, then the total number of iterations becomes 70. Moreover, in every iteration the relative residual, obtained after solving in the dual cells, is higher than the residual obtained after solving the problem in the primal cells. The explanation to that fact is simple - the fine matrix A (i.e. matrix that is obtained after discretizing the problem (2.1) on the fine scale) contains information not only about the solution, but also about its second derivative. Of course, the values of second derivatives are very inaccurate on the boundaries of the cells. The number of boundaries when solving the problem in the primal cells is much less than the number of boundaries

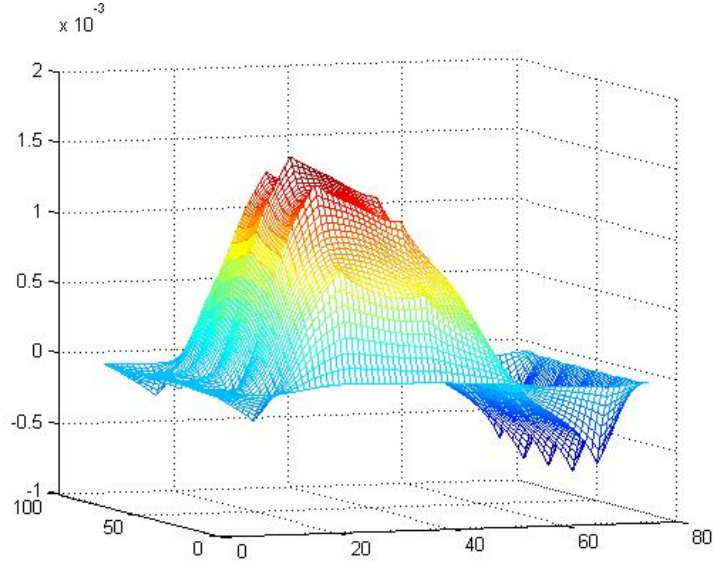


Figure 6.7: The difference between iMSFV solution and the exact solution for the (6.1)-(6.2) system with $[5 \cdot 15 \times 5 \cdot 15]$ grid and 10 smoothing steps in every iMSFV iteration

when solving in the dual cells. This fact leads to the increased value of the relative residual.

On the other hand, the norm between the exact solution and the approximations obtained on every iteration after solving in both primal and dual cells, monotonically decreases. It agrees with the fact, that only the information about second derivatives increases the norm after solving the problem in the dual cells.

If one solves the problem only on primal cells, it takes 73 iterations to reach the desired tolerance. This leads to an interesting conclusion - additive Schwarz on the dual cells does not dramatically increase the rate of convergence comparing to the multiplicative Schwarz in the primal cells, as it was expected. An explanation to this fact lies in the size of the overlap in the multiplicative Schwarz - in the implementation of the method it is always h_x in x -direction and h_y in y -direction. For the example above the overlap is relatively large since $h_x = h_y = \frac{H}{5}$.

Now consider the same example on the domain consisting of $[10 \cdot 15 \times 10 \cdot 15]$ fine cells. Alternating Schwarz method converges to the desired tolerance in 92 iterations, whereas if solving the problem only in the primal cells, the method

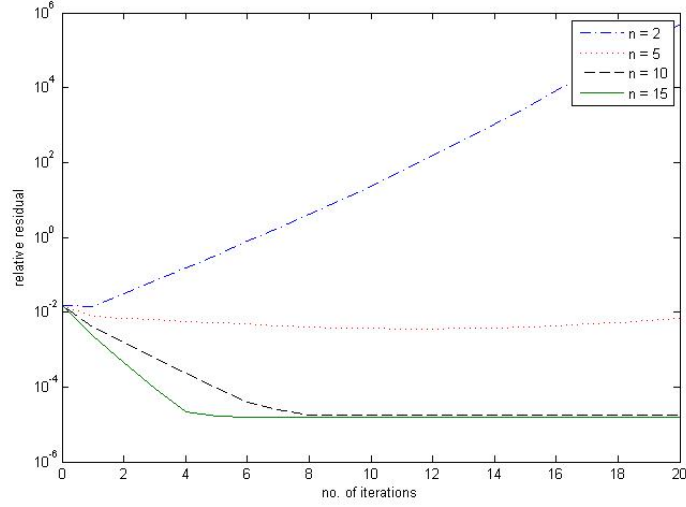


Figure 6.8: Behavior of relative residual with respect to the iteration number for the classical iMSFV method for the (6.1)-(6.2) system with $[5 \cdot 15 \times 5 \cdot 15]$ grid and 2, 5, 10 and 15 smoothing steps

converges to the desired tolerance in 325 iterations, see Figure 6.9. Hence, we can conclude, that the more fine cells constitute the domain of interest, the more crucial becomes solving the equation in the dual coarse cells together with primal coarse cells.

Now consider the system of equations (6.1)-(6.2) and the grid with $[5 \cdot 7 \times 5 \cdot 7]$ fine cells. The method converges in 184 iterations to the required tolerance. In case of performing computations only on primal cells the method converges in 168 iterations. Hence, additive Schwarz on the dual cells even slows down the multiplicative Schwarz on the primal cells, see Figure 6.10. An explanation to this is the same, as for the previous example - the overlap in multiplicative Schwarz is large enough ($h_x = h_y = \frac{H}{7}$), so that there is no need in adding additive Schwarz on dual cells.

Increase the number of fine cells constituting the coarse cell, i.e. consider the grid $[5 \cdot 15 \times 5 \cdot 15]$. Additive Schwarz method for the system (6.1)-(6.2) converges in 238 iterations. In case of performing the method in the primal cells only the method converges in 323 iterations. Hence, the rate of convergence slows down when increasing the number of fine cells per coarse. Moreover, performing additive Schwarz in the dual cells decreases the number of iterations needed for the

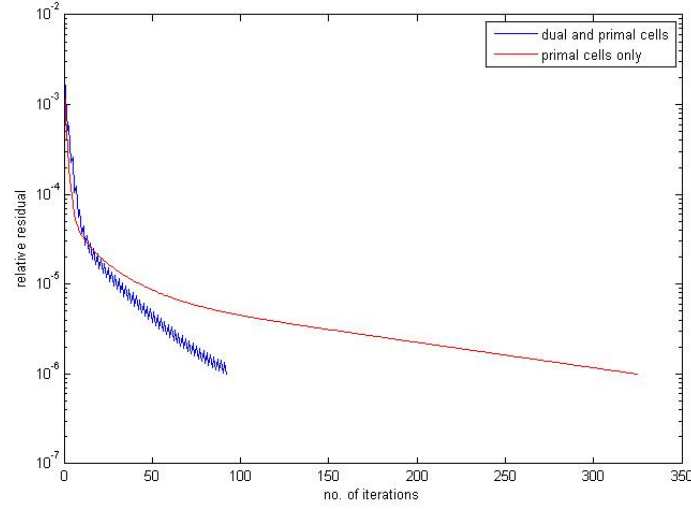


Figure 6.9: Comparison of relative residuals with respect to the iteration number for alternating Schwarz in both dual and primal cells and multiplicative Schwarz in primal coarse cells only, for $[10 \cdot 15 \times 10 \cdot 15]$ grid

convergence, since the overlap in multiplicative Schwarz is much smaller compared to the previous example.

Consider the same problem with the domain consisting of $[10 \cdot 15 \times 10 \cdot 15]$ fine cells, i.e increase the number of coarse cells only. In this case the method converges in 544 iterations. In case of performing the computations only on primal cells the method converges in 705 iterations, see Figure 6.11. The overlap in the multiplicative Schwarz in primal cells is not large enough, hence, as it can be seen from the results, additive Schwarz is necessary on dual cells in order to speed up the convergence. Furthermore, when increasing the number of coarse cells in the domain, leaving the number of fine cells per coarse the same, the number of iterations needed by both methods increases. Hence, additive Schwarz on dual cells and multiplicative Schwarz on primal cells depend both on the number of fine cells and coarse cells constituting the domain.

6.5.2 Multiplicative Schwarz in both dual and primal coarse cells

In this subsection numerical results for multiplicative Schwarz in both dual and primal coarse cells will be presented. Theoretically it should converge much faster,

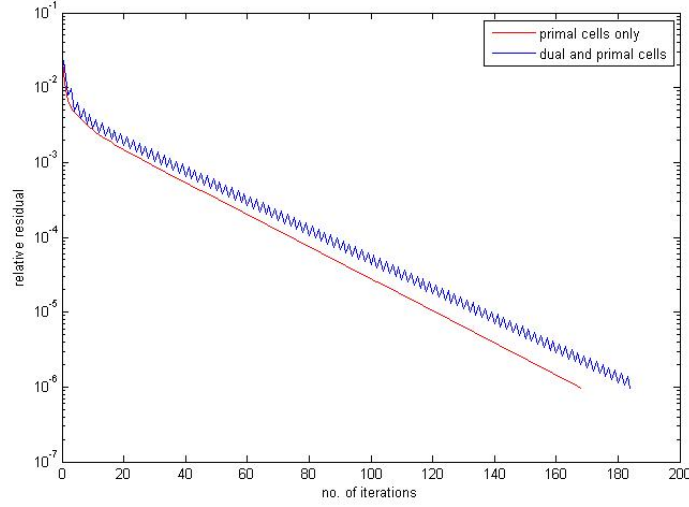


Figure 6.10: Comparison of relative residuals with respect to the iteration number for alternating Schwarz in both dual and primal cells and multiplicative Schwarz in primal coarse cells only, for $[5 \cdot 7 \times 5 \cdot 7]$ grid

than the combination of additive Schwarz on dual cells and multiplicative Schwarz on primal cells.

The system of interest is system (6.1)-(6.2) of equations. The grid is $[5 \cdot 7 \times 5 \cdot 7]$. The desired tolerance is $1 \cdot 10^{-6}$. Multiplicative Schwarz method converges to the tolerance in 123 iterations, which is 1.5 times faster than the combination of additive and multiplicative Schwarz methods. Increase now the number of fine cells per coarse, i.e. consider $[5 \cdot 15 \times 5 \cdot 15]$ grid. The number of iterations needed to converge is 183. Hence, the rate of convergence depends on the number of fine cells per coarse.

If the number of coarse cells is increased, so that the grid consists of $[10 \cdot 15 \times 10 \cdot 15]$ fine cells, then the method converges to the desired tolerance in 402 iterations, see Figure 6.12. Hence, the rate of convergence for the multiplicative Schwarz both in primal and dual cells depends on the number of coarse cells in the grid. However, this method is 1.35 times faster, than the combination of additive and multiplicative Schwarz methods. The relative improvement in the speed of convergence is smaller compared to $[5 \cdot 7 \times 5 \cdot 7]$ grid, since the area of overlap (which is always h_x or h_y) is getting smaller with the increasing number of fine cells.

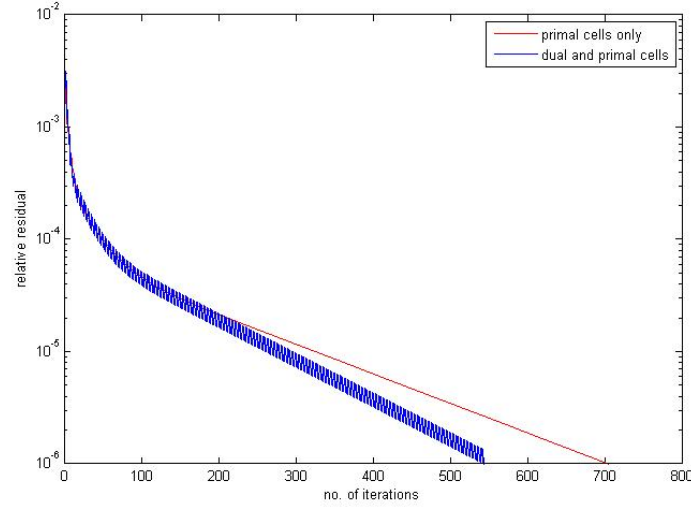


Figure 6.11: Comparison of relative residuals with respect to the iteration number for alternating Schwarz in both dual and primal cells and multiplicative Schwarz in primal coarse cells only, for $[10 \cdot 15 \times 10 \cdot 15]$ grid

6.6 The MSFV method in both dual and primal coarse cells

Consider the system of equations (6.1)-(6.2) and the grid with $[5 \cdot 7 \times 5 \cdot 7]$ fine cells. The desired tolerance is $1 \cdot 10^{-6}$. According to the algorithm described in the corresponding section, the MSFV method is performed in dual and primal coarse cells turn by turn with one step of Gauss-Seidel line relaxation between iterations. For the system above the method converges in only 30 iterations (comparing to 184 for additive Schwarz and 123 for multiplicative Schwarz).

Now consider a grid with the same number of coarse cells, but with increased number of fine cells, i.e. the grid $[5 \cdot 15 \times 5 \cdot 15]$. The iMSFV method for dual and primal cells converges in 120 iterations (for multiplicative Schwarz 183 iterations, for additive 238 iterations). Hence, the convergence rate heavily depends on the number of the fine cells constituting one coarse cell.

Next, the number of fine cells per coarse cell stays the same, but the number of coarse cells is increased to 10 in each direction, i.e. the grid $[10 \cdot 15 \times 10 \cdot 15]$ is considered. The method converges in 121 iterations, hence, the dependence of the convergence of the method on the number of coarse cells is small comparing to the

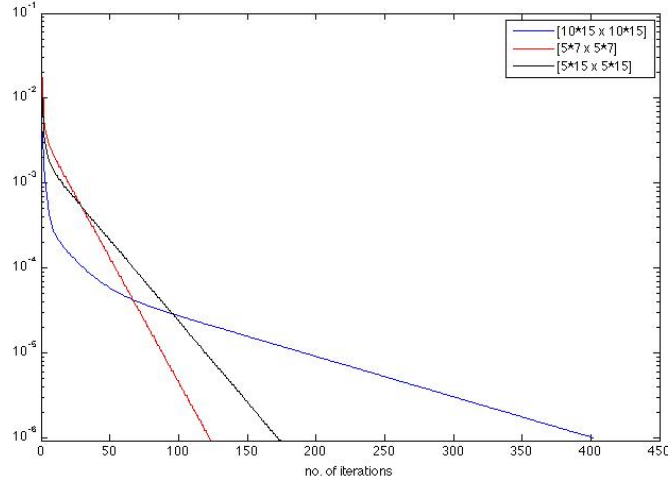


Figure 6.12: Relative residual with respect to the iteration number for multiplicative Schwarz method in both dual and primal coarse cells for different grid sizes

dependence on the number of fine cells per coarse cell. Moreover, the number of iterations needed to converge to the desired tolerance, is significantly lower comparing to the additive (544 iterations) and multiplicative (402 iterations) Schwarz methods. In the Figure 6.13 the dependence of the relative residuals on the iteration number for all 3 types of grid is presented.

Now, consider a number of grids with different amount of fine cells per coarse, but the same amount of coarse cells. This approach will allow to study the dependence of the number of iterations needed for convergence on the number of fine cells constituting the domain. The smallest grid considered is $[5 \cdot 5 \times 5 \cdot 5]$, i.e 5 coarse cells in each direction with 5 fine cells per coarse cell in each direction. Then, the number of fine cells per coarse cell is always increased by 2, since the number of fine cell should be odd. The results are presented in Figure 6.14.

As it can be seen from the figure, the number of iterations linearly depends on the number of fine cells constituting a coarse cell.

Consider now the following system:

$$-\nabla \cdot (53 + 25 \sin(25x) + 25 \sin(25y)) \cdot \nabla p = -1 \quad \text{in } \Omega \quad (6.9)$$

$$p = 0 \quad \text{on } \partial\Omega \quad (6.10)$$

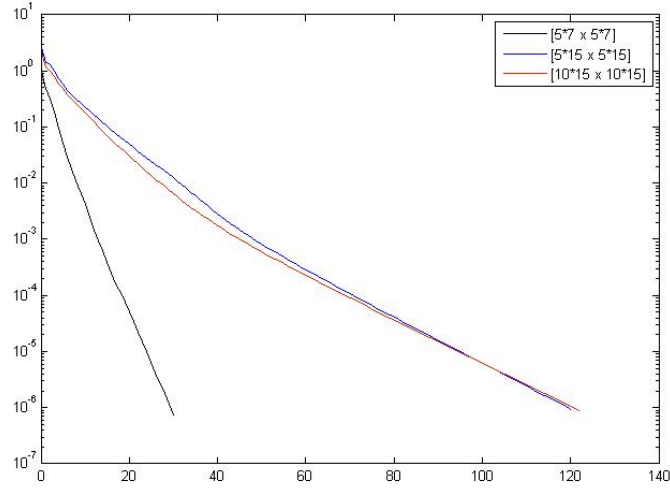


Figure 6.13: Relative residual with respect to the iteration number for iMSFV in dual and primal cells for $[5 \cdot 7 \times 5 \cdot 7]$, $[5 \cdot 15 \times 5 \cdot 15]$ and $[10 \cdot 15 \times 10 \cdot 15]$ grids

The grid is $[10 \cdot 15 \times 10 \cdot 15]$. The method converges to the desired tolerance of $1 \cdot 10^{-6}$ in 128 iterations. In Figure 6.15 relative residual with respect to the iteration number for different methods can be found. As it can be seen, the fastest method is still iMSFV in dual and primal cells, then pcg method for the fine scale discretization (423 iterations), multiplicative Schwarz in both dual and primal cells (898 iterations) and additive Schwarz in dual and multiplicative Schwarz in primal coarse cells (1398 iterations).

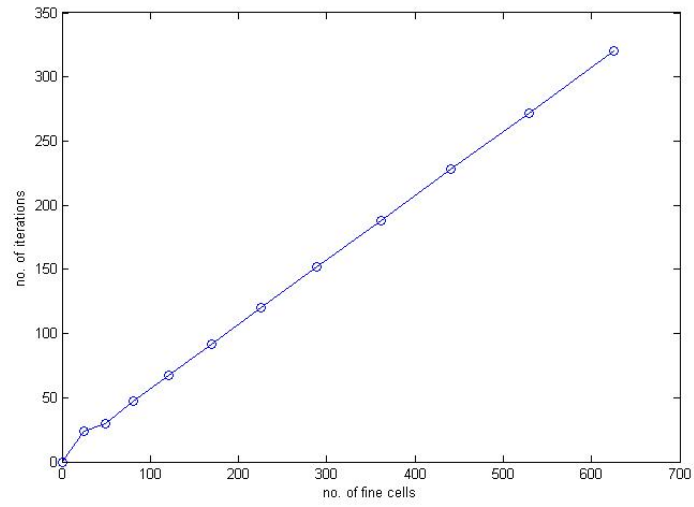


Figure 6.14: Number of iterations with respect to the number of the fine cells per coarse cell

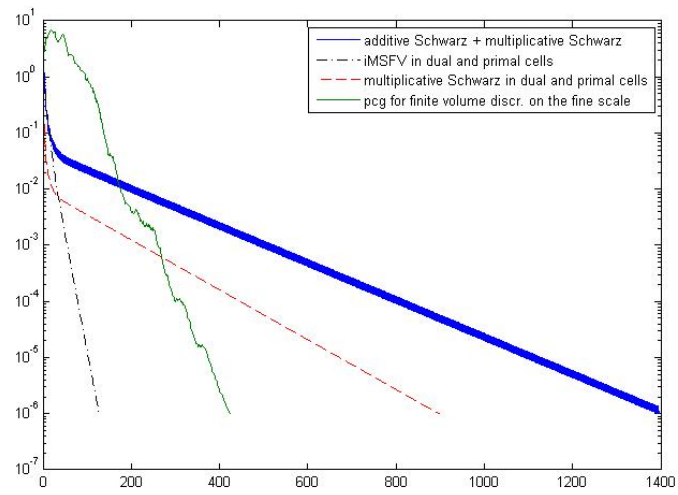


Figure 6.15: Relative residual with respect to the iteration number for various methods

Chapter 7

Conclusions

Several multiscale methods for solving elliptic equations with highly heterogeneous coefficients were implemented. As it can be seen from the previous chapter the best results with the least number of iterations are obtained by the iMSFV which is done both in dual and primal cells. This method, however, requires Jacobi or Gauss-Seidel line relaxation after each iteration and introduction of extra points in the domain of interest to be able to perform calculations in the primal cells. On the other hand, it gives a dramatical decrease in the number of iterations needed to obtain the approximation of the fine scale solution, compared to the classical iMSFV method, alternating Schwarz methods and the FD fine scale discretizations.

As it was shown, the classical MSFV method gives a good approximation of the fine solution, i.e. if one is not interested in the exact solution of the initial problem (2.1), the MSFV method can be performed in order to get satisfying results.

Alternating Schwarz methods can also be used to find the solution of the problem, however, they are slow even compared to the fine difference approximation of the problem on the fine scale. They also depend both on number of coarse cells and primal cells per coarse. Convergence of the iMSFV method in dual and primal cells, however, does not depend on the number of the coarse cells in the domain, but only on the number of fine cells, constituting a coarse cell.

Classical iMSFV heavily depends on the smoothing operations - in some cases, when the smoothing is not sufficient, it may diverge. Normally, several Jacobi or Gauss-Seidel line relaxation steps must be done between the iterations. Hence, this method lacks the stability of the iMSFV method in dual and primal cells, which only needs one line relaxation step between the iterations, and alternating Schwarz methods, which do not require smoothing operations at all. Moreover, as it was shown, at some point it stagnates with the largest error located in the

centers of the primal coarse cells.

The further research can be focused in implementing the methods above, especially the iMSFV method in dual and primal cells, as preconditioners, since now, most of them are implemented as solvers for the fine scale solution of the initial equation (2.1). Moreover, in some cases it is not necessary to update the solution in every point of the domain, hence, it could be useful to update the iMSFV solution only in some areas of the domain, having the criteria for this kind of choice.

Bibliography

- [1] T. Y. Hou and X.-H. Wu. A multiscale finite element method for elliptic problems in composite materials and porous media. *J. Comput. Phys.*, 134:169-189, 1997.
- [2] Z. Chen and T. Y. Hou. A mixed multiscale finite element method for elliptic problems with oscillating coefficients. *Math. Comp.*, 72(242):541-576, 2002.
- [3] J. E. Aarnes, V. Kippe, and K.-A. Lie. Mixed multiscale finite elements and streamline methods for reservoir simulation of large geomodels. *Adv. Water Resour.*, 28(3):257-271, 2005.
- [4] J. E. Aarnes. On the use of a mixed multiscale finite element method for greater flexibility and increased speed or improved accuracy in reservoir simulation. *Multiscale Model. Simul.*, 2(3):421-439, 2004.
- [5] P. Jenny, S. H. Lee, and H. A. Tchelepi. Multi-scale finite-volume method for elliptic problems in subsurface flow simulation. *J. Comput. Phys.*, 187:47-67, 2003.
- [6] H. Hajibeygi and P. Jenny. Multiscale finite-volume method for parabolic problems arising from compressible multiphase flow in porous media. *J. Comput. Phys.*, 228:5129-5147, 2009.
- [7] V. Ginting. Analysis of two-scale finite volume element method for elliptic problem. *J. Numer. Math.*, 12:119-141, 2004.
- [8] H. Hajibeygi, G. Bonfigli, M. A. Hesse and P. Jenny. Iterative multiscale finite-volume method. *J. Comput. Phys.*, 227:8604-8621, 2008.
- [9] J. Bear. Dynamics of fluids in porous media. *Dover Publications*, 1988.
- [10] R. Helmig. Multiphase flow and transport processes in the subsurface: a contribution to the modeling of hydrosystems. *Springer Verlag*, 1997.

- [11] X. H. Wu, Y. Efendiev, T. Y. Hou. Analysis of Upscaling Absolute Permeability, *Discrete and Continuous Dynamical Systems-Series B*, 2(2):185-204, 2002.
- [12] V. Kippe, J. E. Aarnes and K.-A. Lie. A comparison of multiscale methods for elliptic problems in porous media, *J. Comput. Geoscience*, 2007.
- [13] J. M. Nordbotten and P. E. Bjørstad. On the relationship between the multiscale finite-volume method and domain decomposition preconditioners. *J. Comput. Geosciences*, 12(3):367-376, 2008.
- [14] P. Jenny, S. H. Lee, and H. A. Tchelepi. Adaptive multiscale finite-volume method for multiphase flow and transport in porous media. *Multiscale Model. Simul.*, 3(1):50-64, 2004.
- [15] A. St-Cyr, M. J. Gander, and S. J. Thomas. Optimized multiplicative, additive, and restricted additive Schwarz preconditioning. *J. Sci. Comput.*, 29(6):2402-2425, 2007.
- [16] J. E. Aarnes, T. Y. Hou. Multiscale domain decomposition methods for elliptic problems with high aspect ratios. *Acta Mathematicae Applicatae Sinica* 18(1):63-76, 2002.
- [17] S. G. Mikhlin. On the Schwarz algorithm. *Doklady Akademii Nauk SSSR*, 77:569-571, 1951.
- [18] B. F. Smith, P. E. Bjørstad and W. D. Gropp. Domain decomposition: parallel multilevel methods for elliptic partial differential equations, *Cambridge University Press*, 1996.
- [19] G. A. A. Kahoua, E. Kamgniaa, and B. Philippe. An explicit formulation of the multiplicative Schwarz preconditioner. *Applied Num. Math.*, 11-12:1197-1213, 2007.